Strong excitonic effects in $CuAlO_2$ delafossite transparent conductive oxides

Robert Laskowski,[1] Niels Egede Christensen,[2] Peter Blaha,[1] and Balan Palanivel[3]
[1]*Institute of Materials Chemistry, Technische Universität Wien, Getreidemarkt 9/165TC, A-1060 Vienna, Austria*
[2]*Department of Physics and Astronomy, University of Aarhus, DK-8000 Aarhus C, Denmark*
[3]*Department of Physics, Pondicherry Engineering College, Puducherry 605 014, India*
(Received 15 January 2009; revised manuscript received 25 March 2009; published 27 April 2009)

The imaginary part of the dielectric function of $CuAlO_2$ has been calculated including the electron-hole correlation effects within Bethe-Salpeter formalism (BSE). In the initial step of the BSE solver the band structure was calculated within density-functional theory plus an orbital field (LDA/GGA+U) acting on Cu atoms. We discuss the influence of the strength of the additional orbital field on the band structure, electric field gradients, and the dielectric function. The calculated dielectric function shows very strong electron-hole correlation effects manifested with large binding energies of the lowest excitons. The electron-hole pair for the lowest excitations are very strongly localized at a single Cu plane and confined within only a few neighboring shells.

DOI: 10.1103/PhysRevB.79.165209 PACS number(s): 71.15.Qe, 71.35.Cc, 78.20.Ci, 78.40.Fy

I. INTRODUCTION

Delafossite oxides $CuMO_2$, where M is a trivalent metal, belong to the rare class of p-type transparent semiconductors. They are relatively well studied, especially $CuAlO_2$, which was reported to be p-type conducting by Benko and Koffyberg[1] already 25 years ago. They estimated the hole mobility at rather low level of 1.1×10^{-7} m^2/Vs and from electrochemical measurements a lowest indirect band gap of about 1.65 eV was deduced. The compounds attracted more attention after reporting higher p-type electrical conductivity in thin films of $CuAlO_2$ by Kawazoe *et al.*[2] They measured the mobility of holes as high as 10^{-3} m^2/Vs and a conductivity of about 1 S/cm. However in the following work of Yanagi *et al.*[3] the measured value was reduced to 1.3×10^{-4} m^2/Vs. The delafossite ($R\bar{3}m$) unit cell is presented in Fig. 1. It can be viewed as a layered structure, where the Cu cations are linearly coordinated by O and the CuO_2 dumbbells are separated by a layer of edge sharing MO_6 octahedra. Kawazoe *et al.* proposed[2] that the monopolarity in these compounds results from localization of the holes at the oxygen $2p$ levels due to strong electronegativity of the oxygen atoms. Since the energies of the Cu $3d$ orbitals are quite close to the O $2p$ states the strong covalent bonding between Cu and O delocalizes the positive holes.[2,3] At the same time the low-dimensional Cu-O coordination suppresses the interaction and leads to a large band gap comparing to Cu_2O for example. The allowed direct and indirect band gaps were estimated from optical transmission spectra at about 3.5 eV and 1.8 eV.[2,3] Several x-ray spectroscopy studies indicate that both the valence and conduction bands result from strong mixing of Cu $3d$ and O $2p$ states.[3,4] A detailed study of the electronic structure of $CuAlO_2$ has been performed by Aston *et al.* using x-ray photoemission spectroscopy (XPS), x-ray emission spectroscopy (XES), and x-ray absorption spectroscopy (XAS).[4] According to their findings the maximum of the Cu $3d$ band appears about 2.8 eV below the Fermi level, and the maximum of the O $2p$ band is located around 5 eV below it. They also showed a relatively good agreement with *ab-initio* calculations. However the calculated Cu $3d$ band is too close to the valence-band maximum (VBM), its binding energy being only $\approx$1.2 eV. The calculated band structure shows a dispersion of the valence bands around the F and L points mainly due to the interaction between Cu d_{z^2} and O p_z states,[5] whereas relatively flat bands around Γ and Z originate from antibonding Cu-O π states. The series of $CuMO_2$ delafossites, where M is Al, Ga, or In shows band-gap anomalies. The optically measured gaps are 3.5 eV for $CuAlO_2$, 3.6 eV for $CuGaO_2$, and 3.9 for $CuInO_2$. This trend contradicts observed trends for other group-III containing semiconductors. Using first-principles methods Nie *et al.*[6] gave a simple explanation of this anomaly. They found that the direct gaps follow the general trend and decrease within the series, however the region of the Brillouin zone (BZ) around Γ is optically inactive. It happens that for $CuInO_2$ and $CuGaO_2$ the fundamental gaps are at Γ, whereas the optical allowed transitions start at higher energies around L.

The electron-hole correlation can strongly affect the calculated optical response of a material. The strength of such effects depends to some extent on the atomic structure of a compound. Layered structures enhance the localization of the electron-hole pairs and lead to a strong electron-hole interaction. From a point of view of a band structure, parallel valence and conduction bands lead often to delocalized excitons in k space and therefore allows for their real-space localization. Due to their layered structure and their band structure the delafossites are expected to be materials where the electron-hole correlations are rather strong. In this work we explicitly calculate the optical spectra including the electron-hole correlation by solving the Bethe-Salpeter equation (BSE). We analyze the lowest excitons in real as well as in k space. Since the electron-electron correlation within the Cu atom is also an interesting issue and certainly affects the band structure of $CuAlO_2$, we also analyze it within standard density-functional theory plus an orbital field (LDA/GGA+U) (Refs. 7–9) methodology.

II. COMPUTATIONAL METHOD

The scheme for calculating the optical response including the electron-hole interactions used in this work is based on

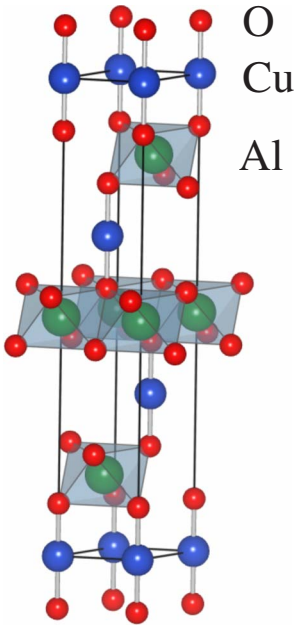

FIG. 1. (Color online) The structure of $CuAlO_2$. The lattice parameters of the conventional unit cell are set to 2.858 Å and 16.958 Å for a and c respectively. The distance between Cu and O atoms in the dumbbell is set to 1.864 Å.

the solution of the equation of motion of the two-particle Green's function, known as the Bethe-Salpeter equation.[10] A detailed discussion concerning various aspect of the BSE formalism, as well alternative approach employing time-dependent density-functional theory (TDDFT) can be found in Ref. 11. The computational procedure solves this equation in an approximate manner represented in the form of an effective eigenvalue problem with the BSE Hamiltonian[12–16]

$$\sum_{v'c'\mathbf{k}'} H^{e}_{vc\mathbf{k},v'c'\mathbf{k}'} A^{\lambda}_{v'c'\mathbf{k}'} = E^{\lambda} A^{\lambda}_{vc\mathbf{k}}. \tag{1}$$

The equation is formulated in the basis of electron and hole quasiparticle states, $vc\mathbf{k}$ denotes an elementary excitation taking place at a point $\mathbf{k}$ of the BZ, from a valence (v) to a conduction (c) band. The excitation spectrum is given by the eigenvalues of this equation. Therefore the excitons are a linear combination of "elementary" excitations. The excitonic correlation function is defined by the equation

$$\Phi^{\lambda}(\mathbf{r}_e, \mathbf{r}_h) = \sum_{vc\mathbf{k}} A^{\lambda}_{vc\mathbf{k}} \psi^{*}_{v\mathbf{k}}(\mathbf{r}_h) \psi_{c\mathbf{k}}(\mathbf{r}_e). \tag{2}$$

In this formalism only direct transitions leading to excited states with infinite lifetime are considered, assuming the absence of exciton-phonon coupling. The exciton-phonon interaction mixes the excitons with the indirect optical transitions. Such interaction is rather difficult to include in a general fashion. However it was included into the BSE formalism and applied for carbon nanotubes.[17] BSE was formulated there in a basis of tight-binding Hamiltonian including a model for electron-phonon interactions. The effective BSE Hamiltonian is a sum of three terms,

$$H^{e} = H^{\mathrm{diag}} + H^{\mathrm{dir}} + H^{x}, \tag{3}$$

which are defined as

$$H^{\mathrm{diag}}_{vc\mathbf{k},v'c'\mathbf{k}'} = (\varepsilon_{c\mathbf{k}} - \varepsilon_{v\mathbf{k}} + \Delta)\delta_{vv'}\delta_{cc'}\delta_{\mathbf{k}\mathbf{k}'}, \tag{4}$$

$$H^{\mathrm{dir}}_{vc\mathbf{k},v'c'\mathbf{k}'} = -\int \mathrm{d}^3 r \mathrm{d}^3 r' \psi_{v\mathbf{k}}(\mathbf{r}) \psi^{*}_{c\mathbf{k}}(\mathbf{r}') \times W(\mathbf{r},\mathbf{r}') \psi^{*}_{v'\mathbf{k}'}(\mathbf{r}) \psi_{c'\mathbf{k}'}(\mathbf{r}'), \tag{5}$$

$$H^{x}_{vc\mathbf{k},v'c'\mathbf{k}'} = \int \mathrm{d}^3 r \mathrm{d}^3 r' \psi_{v\mathbf{k}}(\mathbf{r}) \psi^{*}_{c\mathbf{k}}(\mathbf{r}) \times \bar{v}(\mathbf{r},\mathbf{r}') \psi^{*}_{v'\mathbf{k}'}(\mathbf{r}') \psi_{c'\mathbf{k}'}(\mathbf{r}'). \tag{6}$$

The direct-interaction term H^{dir} describes the screened Coulomb attraction (W) between the hole and the electron. The necessary dielectric matrix is calculated within the random-phase approximation (RPA) including local-field effects.[18,19] The term H^{x} accounts for exchange interaction between electron and hole and involves only short-range part of the bar Coulomb interaction ($\bar{v}$). Neglecting the direct and exchange terms leaves only the diagonal part of the Hamiltonian (H^{diag}) and results in the independent electron-hole approximation. The quasiparticle states, which are the basis of the BSE Hamiltonian, are well approximated by density functional theory (DFT) wave functions,[20] but the conduction-band energies are often too close to the VBM. Usual practice in such a situation is to construct the BSE Hamiltonian directly using the DFT wave vectors. The self-energy is approximated either by an appropriate rigid shift of the conduction bands, determined by adjusting the DFT band gap to the measured value at ambient conditions, or by an application of so-called GW approximation[21–24] to the self-energy, which is methodologically more consistent, as the BSE equations are derived using this approximation. However this approach is much more computationally expensive and the non-self-consistent version of it combined with full-potential method does not improve the band energies as much as it is observed for pseudopotential methods.[25] As we will show for $CuAlO_2$, our calculated direct band gap [using generalized gradient approximation plus orbital potential (GGA+U) method] is very close to the measured optical band gap of 3.5 eV (estimated from optical transmission[2,3]). Therefore we decided to use directly the GGA+U eigenvalues as the quasiparticle energies. The GGA+U eigenstates are used consistently at all steps of the BSE Hamiltonian setup, including the calculation of RPA screening of the electron-hole interaction.

The linearized augmented plane wave plus local orbitals (LAPW+LO) method as implemented in WIEN2K program[26] was used to calculate the single-particle states. The implementation of the BSE scheme within the linearized augmented plane wave (LAPW) method has already been applied to centrosymmetric[27,28] and noncentrosymmetric[29,30] systems. The DFT calculations were performed with the Perdew, Burke, and Ernzerhof parameterization of the GGA of the exchange-correlation potential.[31] An important issue in the calculation is the density of the k mesh applied to de-

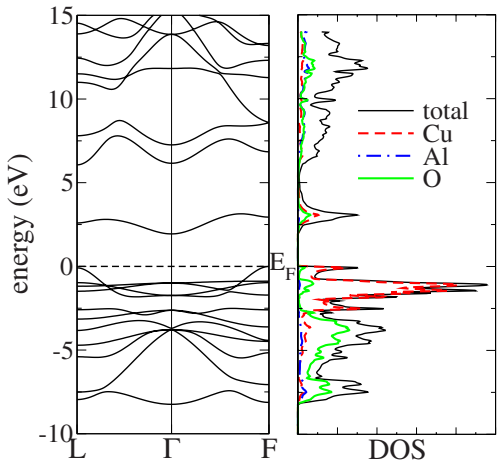

FIG. 2. (Color online) The band structure and the corresponding DOS calculated with GGA.

scribe the correlation function coefficients $A^{\lambda}_{vc\mathbf{k}}$. In most cases the desired density is very high, and this makes the BSE Hamiltonian extremely expensive to construct. In order to overcome this difficulty we employed an "interpolation technique."[16] The method simply operates on two k meshes, one with a low and another one with a high k-point density. In the first stage the exact BSE Hamiltonian is computed on the low-density mesh. Then, on the dense mesh the elements of the final BSE Hamiltonian are calculated using a much simpler interpolation formula. Tests have shown that the errors due to the interpolation are marginal, and that it significantly speeds up the setup of the BSE Hamiltonian. In this work we have performed two sets of BSE calculations. In the first one we compute the imaginary part of the dielectric function. In this case a moderately dense k mesh gives converged results. We use a $4\times4\times4$ regular grid (for the rhombohedral unit cell) as the low-density mesh and a $12\times12\times12$ grid as the high-density mesh. In this case the number of valence and conduction bands that enter the BSE Hamiltonian must be large enough to cover the relatively wide range of photon energies. In order to cover a range of 10 eV we use 12 valence and four conduction bands. In the second set of calculations we focused on the lowest excitons only. In order to precisely calculate their binding energies we have doubled both the k meshes and use $8\times8\times8$ for the low-density one and $24\times24\times24$ for the high-density k mesh. Since the excitons are formed almost exclusively out of transitions from the top of the valence to the bottom of the conduction bands we can use here only four valence and one conduction bands.

III. RESULTS

The DFT-calculated band structure of $CuAlO_2$ delafossites has already been discussed in the literature.[3,5,6] However for clarity of the presentation we show in Fig. 2 our GGA band structure and density of states (DOS). The lowest conduction band forms a well-isolated DOS peak with mainly Cu-d_{z^2} and O-p_z character, and only a minor admixture of O-s and O-$p_{x,y}$. The valence-band edge together with the first valence DOS peak originates from states around the L and F points of the BZ, which are almost exclusively of Cu-d_{z^2} and O-p_z character. The most pronounced second DOS peak is related to the flat valence bands that are on the band edge around Γ. It is composed mainly of Cu-d_{xy} and Cu-d_{xz} with an admixture of O-$p_{x,y}$ states. The lower part of the DOS is dominated by O-$p_{x,y}$ character. Considering the linear character of the Cu-O chains the observed dispersive Cu-d_{z^2}-O-p_z bands and flat Cu-d_{xy}, d_{xz} bands seems to be rather natural. It is well known that DFT tends to place the 3d states too close to the Fermi level due to the self-interaction error. In the case of $CuAlO_2$ the maximum of the Cu-3d DOS appears at about 1.2 eV (see Fig. 2) below the VBM. The XPS of Aston *et al.*[4] indicates its position at about 2.8 eV. Such deficiency can be corrected in a very simple and efficient way by applying the LDA/GGA+U formalism.[7–9] The Cu ion has an almost full 3d shell which we would like to move down in energy. Therefore we chose the Anisimov *et al.*[7] version of double counting (fully localized limit). In a simplified picture the orbital potential applied to the d shell of the Cu ion has a form

$$V^{\mathrm{FLL}} = (U-J)\left(\frac{1}{2}-\hat{n}_{\sigma}\right), \tag{7}$$

where $\hat{n}_{\sigma}$ gives the occupancy of the orbital σ. In order to avoid double counting in the nonspherical part of the potential, an effective Hubbard U, $U_{\mathrm{eff}}=U-J$ is used instead of separate U and J, and also the multipolar term proportional to J in the LDA+U potential is omitted. As we can see in Fig. 3 the potential V^{FLL} shifts the center of gravity of the d states toward lower energies. The shift is proportional to the value of U_{eff}. For pure GGA calculations the maximum of the Cu-3d DOS appears at 1.2 eV below the Fermi level and for U_{eff} equal to 13.6 eV the maximum is shifted to 3 eV below the Fermi level. For U close to 8 eV the position of the Cu-3d peak matches experimental (Fig. 3). Due to the strong hybridization between the Cu-3d and the O-p states the change of the d band position also affects the band gaps. As shown in Fig. 4 the direct and indirect gaps, except the one at Γ, increase monotonically with U. The gap at Γ reaches its maximum for U equal to 11 eV. The lowest direct transition appears at the L point, except for U greater then 12 eV where the transition at Γ is the lowest one. The order of the indirect gaps between F-Γ and L-Γ does not change with U, however both are relatively close to each other. The experimentally estimated lowest direct and indirect gaps are about 3.5 and 1.8 eV, respectively. GGA calculations underestimate the direct gap ($U=0$ eV) as expected. The GGA+U calculations move it in the right direction, such that for U equals 8 eV the lowest gap reaches the experimental value, when we neglect the decrease in the direct gap due to the exciton binding energy. The indirect transitions are overestimated by about 0.5 eV for that value of U. The applied orbital field enforces localization of the Cu-3d shell which affects the intra atomic charge distribution. The electric field gradients (EFG) is a quantity sensitive to the anisotropy of the charge distribution close to the nucleus, therefore it is sensitive to the strength of the orbital potential. Moreover it

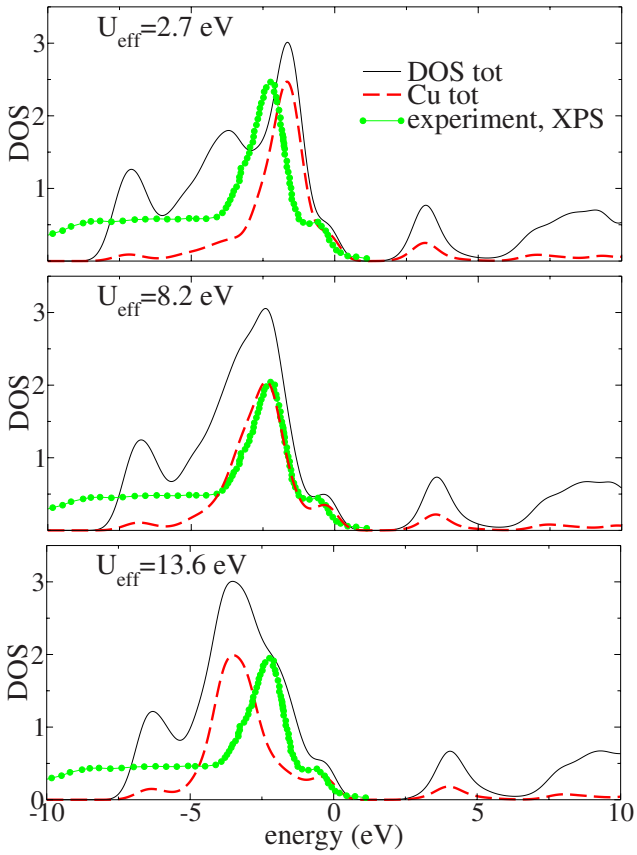

FIG. 3. (Color online) DOS calculated with different values of U_{eff} compared with experimental XPS (Ref. 4). The DOS are plotted with Gaussian broadening of 0.35 eV equal to the instrument resolution used by Aston *et al.* (Ref. 4). The experimental XPS has been shifted by 0.4 eV in order to align it with the valence-band edge of the calculated DOS.

can be easily calculated within the LAPW method[32,33] by $V_{zz} \propto \int \frac{\rho(r) Y_{20}}{r^3} dr$. For further analysis the charge density $\rho(r)$ can be decomposed into different angular-momentum contributions in order to trace back which orbitals contribute to the EFG. Most important in our case are the *p*-*p* and *d*-*d* contributions which are proportional to the respective partial charges as $V_{zz}^{p-p} \propto \langle \frac{1}{r^3} \rangle_p [1/2(p_x + p_y) - p_z]$ and $V_{zz}^{d-d} \propto \langle \frac{1}{r^3} \rangle_d [(d_{xy}$

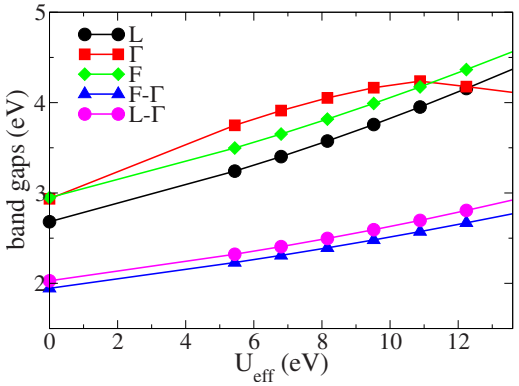

FIG. 4. (Color online) The dependency of direct and indirect band gaps on the U_{eff} parameter.

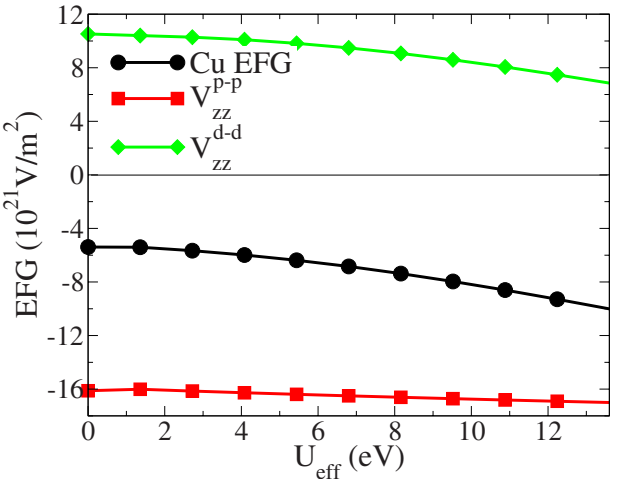

FIG. 5. (Color online) The dependency of the Cu-EFG, and the main components (V_{zz}^{d-d} and V_{zz}^{p-p}) on the value of U_{eff}.

$+d_{x^2-y^2}) - 1/2(d_{xz} + d_{yz}) - d_{z^2}]$. The variation of the total EFG and the *p*-*p* and *d*-*d* components with U_{eff} are shown in Fig. 5. The absolute value of the EFG increases with the strength of the orbital field. Most of this change is due to the *d*-*d* component, which decreases its absolute value with an increase in U_{eff}. The effect is related to the increased occupation of the 3*d* shell forced by the orbital potential, which makes the charge distribution of the 3*d* shell more spherical, when accommodating an increased number of electrons. The GGA calculations result in an EFG of about -5×10^{21} V/m^2, which is only half of the experimental value of 10.6×10^{21} V/m^2 (only the magnitude of the EFG can be measured).[34] However, with GGA+*U* and a large U_{eff} equal to 13.6 eV the calculated value (-10×10^{21} V/m^2) comes close to the experimental EFG.

Considering our results it is rather clear that the GGA +*U* method improves the electronic structure compared to calculations with GGA only. The position of the Cu 3*d* DOS, the band gaps and the value of the EFG on the Cu site are much closer to the experimental values. There is however an open question concerning the value of the parameter *U*. Our results suggest the use of U_{eff} in the range of 8 to 13 eV. Solovyev *et al.*[35] calculated *U* for LaMO$_3$(M=Ti-Cu) for *M* in 2+ and 3+ valence states using the standard constrained L(S)DA technique. Their values for divalent and trivalent Cu ions are close to 9 and 10 eV, respectively. However in our case the valency of the Cu ion is between +1 and +2, with slightly more than nine *d* electrons inside an atomic sphere of 2.064 Å diameter. Therefore a smaller value then 9 eV should be adopted for *U* in our case. The calculated exchange parameter *J* is close to 1 eV for the whole series of LaMO$_3$.[35] This gives us the estimate for U_{eff} of about 8 eV, which is used for further calculations of the absorption spectra. Applying higher values will not change the resulting spectra considerably apart from increasing the band gaps.

The imaginary part of the dielectric function (ε_2) calculated within BSE/GGA+*U*, GGA+*U*, and GGA are presented in Fig. 6. In addition Fig. 7 contains a spatial partitioning of ε_2 calculated within GGA. The contributions related to the particular regions specified in the Fig. 7

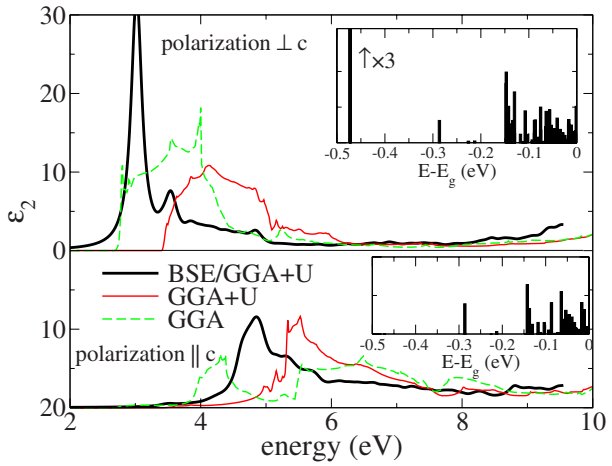

FIG. 6. (Color online) The imaginary part of the dielectric function ε_2 calculated with GGA, GGA+U, and BSE/GGA+U. The inset shows the distribution and the spectral weight of the excitonic levels inside the band gap. For GGA+U the band structure was calculated with U_{eff}=8 eV.

(atomic spheres or interstitial region) have been derived from momentum matrix elements calculated by including only those regions. Note that the expression for the dielectric function involves the square of the momentum matrix elements. Therefore the sum of the contributions may not result in the total spectra depending on the strength of the cross terms. Anyway, in the current case we find such partitioning useful and informative for the analysis of the spectra. Our GGA results are very close to earlier published theoretical spectra.[5,6] The dielectric function shows significant anisotropy of its components perpendicular and parallel to the c axis. The ε_2 calculated for polarization perpendicular to c is dominated by a broad peak that extends between an absorption edge at 2.75 and 4.4 eV, slowly decaying for higher energies. As we see in Fig. 7 this peak can be attributed mainly to an oscillator strength from the Cu atomic sphere. The absorption edge corresponds to transitions around the F and L k points with Cu-3d_{z^2} character at the top of the valence bands to the first conduction band which has significant

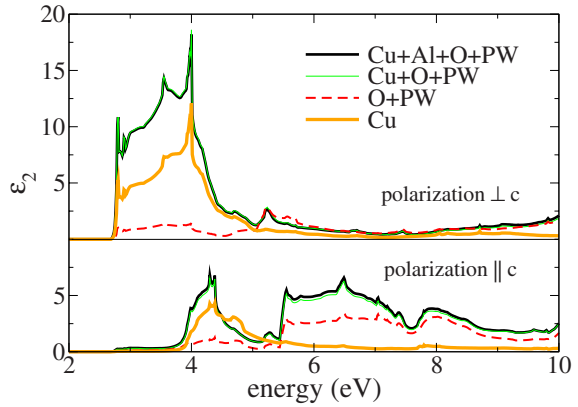

FIG. 7. (Color online) The spatial partitioning of the imaginary part of the dielectric function calculated with GGA. The atomic symbols in the legend indicate contributions from corresponding atomic spheres, PW stands for the plane-wave region.

Cu-$p_{x,y}$ character. The upper edge of the peak (around 4 eV) is due to transitions from lower valence states (Cu-O π states) to the first conduction band. The spectrum calculated for parallel polarization consists of two peaks. The first one between 3.9 and 4.8 eV shows a broad shoulder starting at 2.75 eV and can be related to Cu atom (see Fig. 7). It originates from transitions between Cu-O π states to the first conduction band. The second absorption peak extending from 5.4 eV is related to transition associated with the O spheres and interstitial region. The effect of the GGA+U orbital field on the dielectric function for perpendicular polarization manifests itself as an almost rigid shift of 0.8 eV, which is rather obvious since all transitions involve states with Cu 3d character. For the parallel polarization only the lower peak relates to transitions from states with Cu 3d character; therefore only this peak is shifted to high energies and consequently overlapping with the second peak. Thus for $\varepsilon_2^{\parallel}$ GGA+U does not result in a simple rigid shift, but the shape of $\varepsilon_2^{\parallel}$ is modified. As we can see in Fig. 6 the electron-hole correlations included in the BSE/GGA+U calculations shifts the absorption peaks down in the energy scale. In the case of parallel polarization this results in an almost rigid shift of about 0.6 eV. For the perpendicular polarization, however, the dielectric function is also modified significantly with a lot of weight moved into the absorption edge. The spectrum is composed of two well-separated peaks, with the first peak at 3.0 eV and the second at 3.5 eV. The inset in Fig. 6 shows that the first peak comes from a single excitonic level, whereas the second peak gathers the oscillator strengths of several excitations. Note that the inset in Fig. 6 shows the excitonic levels calculated with the dense k mesh ($24\times24\times24$), while the whole spectrum was calculated with the smaller k mesh ($12\times12\times12$). The binding energy of the lowest excitonic state (defined as the difference between the band gap and the excitation energy) calculated with a dense k mesh is equal to 0.47 and 0.28 eV for perpendicular and parallel polarization, respectively. However the oscillator strength of the parallel polarized exciton is very small and can hardly contribute to the dielectric function. The next excitation has a binding energy close to 0.15 eV for both polarizations. Such high value of the binding energy of the lowest excitons is related to the localization of the excitonic correlation function [Eq. (2)] in real space and the corresponding delocalization in reciprocal space. Figure 8 presents the k-space distribution of the $A^{\lambda}_{vc\mathbf{k}}$ coefficients for the lowest excitonic state of both polarizations. In both cases the correlation function is composed almost exclusively of transitions between the topmost valence and the lowest conduction states. The left part of Fig. 8 shows the three-dimensional isosurface of A_{vck} within the primitive BZ. The right part shows the two-dimensional distribution in a plane shown on the left figure where each k point is indicated with a dot, and the size of the dots is proportional to the corresponding absolute value of A_{vck} (weight). For both polarizations the weights are concentrated around L and F k points and essentially no transitions occur at the center of the BZ. The real-space distribution of the correlation function is presented in Fig. 9. The dots indicate the periodic images of the rhombohedral unit cell in the plane perpendicular to the hexagonal-c direction, the size of the dots are proportional to

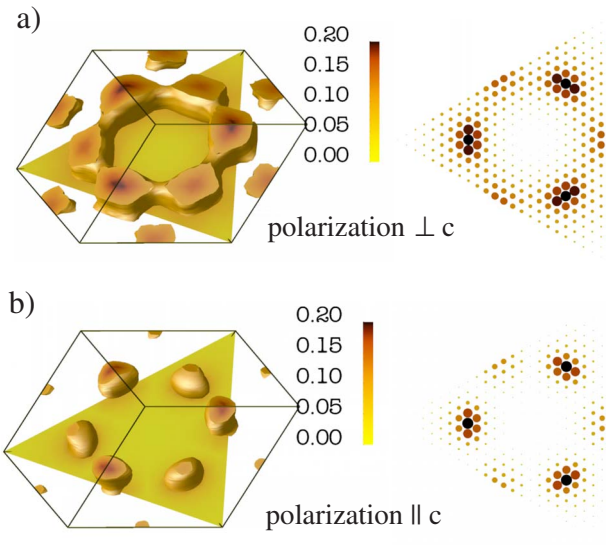

FIG. 8. (Color online) The distribution of the correlation function $A_{v,c,k}$ in the BZ calculated for lowest lying excitons for polarization perpendicular and parallel to the c axis. Only topmost valence and lowest conduction-band contribution is shown. The left part shows the three-dimensional isosurface of A_{vck} within the primitive BZ. The right part shows the two-dimensional distribution on a plane indicated on the left figure where each k point is marked with a dot, the size of the dots is proportional to the absolute values of A_{vck}.

the probability of finding a hole inside a Cu atomic sphere assuming that an electron is inside the central Cu atomic sphere (Cu-Cu). The Cu-O (a hole on Cu, an electron on the central O) and O-Cu (a hole on O, an electron on the central Cu) have similar probability distribution shape; however they are six and ten times smaller. Other combinations do not contribute significantly to the total probability distribution. The excitons for both polarizations are almost perfectly confined within a Cu-O plane. In the case of perpendicular polarization [Fig. 9(a)] the maximum of the probability distribution occurs at the origin (electron and hole are on the same Cu atom) and decays very fast, vanishing after the second coordination shell. In the case of the parallel exciton the

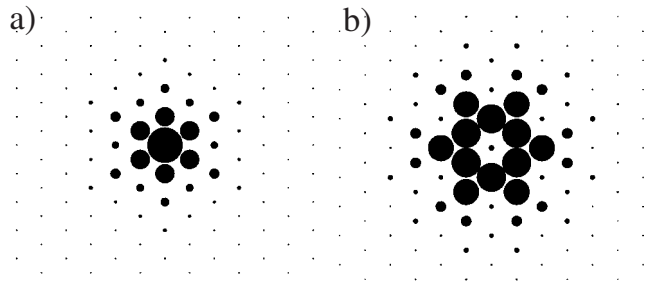

FIG. 9. The real-space distribution of the lowest excitons. (a) shows the distribution calculated for perpendicular polarization, (b) for parallel. The dots indicate the periodic images of the rhombohedral unit cell in the plane perpendicular to the hexagonal-c direction, the size of the dots are proportional to the probability of finding a hole inside Cu atomic sphere assuming that an electron is inside the central Cu atomic sphere (Cu-Cu).

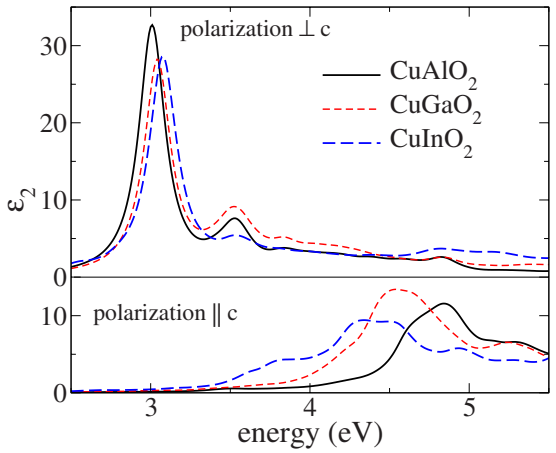

FIG. 10. (Color online) The Imaginary part of the dielectric function calculated with BSE/GGA+U for $CuAlO_2$, $CuGaO_2$, and $CuInO_2$. For all materials the band structure was calculated with U_{eff}=8 eV.

probability of finding an electron and a hole on the same atom is very small, but it is considerable in the first and the second coordination shell and after that decays quickly after the third shell.

The absorption edge in $CuAlO_2$ is formed by excitations which are active for perpendicular polarization only (see Fig. 6). Our BSE/GGA+U value is close to 3.0 eV, whereas the experimentally estimated gap is about 3.5 eV.[2,3] Note that the gap calculated within GGA+U is bigger by the exciton binding energy and almost perfectly fits to the experimental value. The 0.5 eV disagreement can be compensated using a bigger value of U_{eff}, as we have already discussed above (see Fig. 4). A value of U_{eff} of 11 eV results in a L gap close to 4.0 eV. The corresponding change in the electronic structure does not affect noticeably the excitonic binding energies; therefore the absorption gap would be close to 3.5 eV.

Using a similar approach as for $CuAlO_2$ we have performed calculations of the absorption spectra of $CuGaO_2$ and $CuInO_2$. Since the series of $CuMO_2$ compounds, where M = Al, Ga, In has been earlier a subject of discussion concerning the band-gap order[6] it is interesting to see whether the electron-hole correlation affects the predicted absorption gaps. As we can see in Fig. 10 the spectra calculated for all three compounds exhibit similar features. In all cases we used GGA+U with U equal to 8 eV. The absorption edge is active for parallel polarization only. The positions of the first absorption peaks increases in the order of $CuAlO_2$ (3.0 eV), $CuGaO_2$ (3.04 eV), and $CuInO_2$ (3.08 eV). The calculated ordering agrees with the experimentally observed absorption gaps: 3.5 eV ($CuAlO_2$), 3.6 eV ($CuGaO_2$), and 3.9 eV ($CuInO_2$); however the differences between the calculated gaps are much smaller.

IV. CONCLUSIONS

To summarize, we have calculated the imaginary part of the dielectric function of $CuAlO_2$ including electron-hole correlations within the framework of DFT/BSE theory. In order to correct known deficiencies of traditional DFT with

GGA or LDA we have applied an orbital potential in the form of the GGA+U method (at this point we do not expect any fundamental differences with LDA+U approach). First we tried to establish the appropriate value of the U_{eff} parameter by analyzing its effect on DFT band gaps and electric field gradient on the Cu site. In both cases the additional orbital potential pushes the Cu-d bands down in energy modifying the interaction with oxygen. In summary, increasing U_{eff} results in an increase in all gaps as well as an increase in the absolute value of the EFG. This motivates the use of a U_{eff} close to 8 eV, which agrees with the values suggested by Solovyev *et al.*[35] The effect of the orbital potential on the dielectric function calculated within DFT is correlated with the changes of the position of the Cu 3d states. For perpendicular polarization it is nearly a rigid shift, whereas for parallel polarization only the first peak of the spectra shifts and overlaps with the second peak. Finally our BSE calculations performed with the GGA+U band structure shows very strong electron-hole correlation effects, with the lowest exciton binding energy of the order of 0.47 eV for perpendicular polarization. Such a high value results from the strong localization of the exciton within the Cu plane perpendicular to the hexagonal axis of the unit cell.

ACKNOWLEDGMENTS

This work was supported by the Austrian Science Fund under Contract No. P20271-N17.

[1] F. A. Benko and F. P. Koffyberg, J. Phys. Chem. Solids **45**, 57 (1984).
[2] H. Kawazoe, M. Yasukawa, H. Hyodo, M. Kurita, H. Yanagi, and H. Hosono, Nature (London) **389**, 939 (1997).
[3] H. Yanagi, S. Inoue, K. Ueda, H. Kawazoe, and H. Hosono, J. Appl. Phys. **88**, 4159 (2000).
[4] D. J. Aston, D. J. Payne, A. J. H. Green, R. G. Egdell, D. S. L. Law, J. Guo, P. A. Glans, T. Learmonth, and K. E. Smith, Phys. Rev. B **72**, 195115 (2005).
[5] B. J. Ingram, T. O. Mason, R. Asahi, K. T. Park, and A. J. Freeman, Phys. Rev. B **64**, 155114 (2001).
[6] X. Nie, S.-H. Wei, and S. B. Zhang, Phys. Rev. Lett. **88**, 066405 (2002).
[7] V. I. Anisimov, I. V. Solovyev, M. A. Korotin, M. T. Czyżyk, and G. A. Sawatzky, Phys. Rev. B **48**, 16929 (1993).
[8] M. T. Czyżyk and G. A. Sawatzky, Phys. Rev. B **49**, 14211 (1994).
[9] V. I. Anisimov, J. Zaanen, and O. K. Andersen, Phys. Rev. B **44**, 943 (1991).
[10] L. J. Sham and T. M. Rice, Phys. Rev. **144**, 708 (1966).
[11] G. Onida, L. Reining, and A. Rubio, Rev. Mod. Phys. **74**, 601 (2002).
[12] G. Strinati, Phys. Rev. Lett. **49**, 1519 (1982).
[13] G. Strinati, Phys. Rev. B **29**, 5718 (1984).
[14] S. Albrecht, L. Reining, R. Del Sole, and G. Onida, Phys. Rev. Lett. **80**, 4510 (1998).
[15] L. X. Benedict, E. L. Shirley, and R. B. Bohn, Phys. Rev. Lett. **80**, 4514 (1998).
[16] M. Rohlfing and S. G. Louie, Phys. Rev. Lett. **81**, 2312 (1998).
[17] V. Perebeinos, J. Tersoff, and P. Avouris, Phys. Rev. Lett. **94**, 027402 (2005).
[18] S. L. Adler, Phys. Rev. **126**, 413 (1962).
[19] N. Wiser, Phys. Rev. **129**, 62 (1963).
[20] M. S. Hybertsen and S. G. Louie, Phys. Rev. B **34**, 5390 (1986).
[21] M. S. Hybertsen and S. G. Louie, Phys. Rev. B **32**, 7005 (1985).
[22] R. W. Godby, M. Schlüter, and L. J. Sham, Phys. Rev. B **35**, 4170 (1987).
[23] L. Hedin, Phys. Rev. **139**, A796 (1965).
[24] L. Hedin, J. Phys.: Condens. Matter **11**, R489 (1999).
[25] R. Gómez-Abal, X. Li, M. Scheffler, and C. Ambrosch-Draxl, Phys. Rev. Lett. **101**, 106404 (2008).
[26] P. Blaha, K. Schwarz, G. K. H. Madsen, D. Kvasnicka, and J. Luitz, *WIEN2k, An Augmented Plane Wave Plus Local Orbitals Program for Calculating Crystal Properties* (Vienna University of Technology, Austria, 2001).
[27] P. Puschnig and C. Ambrosch-Draxl, Phys. Rev. B **66**, 165105 (2002).
[28] P. Puschnig and C. Ambrosch-Draxl, Phys. Rev. Lett. **89**, 056405 (2002).
[29] R. Laskowski and N. E. Christensen, Phys. Rev. B **74**, 075203 (2006).
[30] R. Laskowski and N. E. Christensen, Phys. Rev. B **73**, 045201 (2006).
[31] J. P. Perdew, K. Burke, and M. Ernzerhof, Phys. Rev. Lett. **77**, 3865 (1996).
[32] P. Blaha, K. Schwarz, and P. H. Dederichs, Phys. Rev. B **37**, 2792 (1988).
[33] P. Blaha, K. Schwarz, W. Faber, and J. Luitz, Hyperfine Interact. **126**, 389 (2000).
[34] R. Abdullin, V. Kal'chev, and I. Pen'kov, Phys. Chem. Miner. **14**, 258 (1987).
[35] I. Solovyev, N. Hamada, and K. Terakura, Phys. Rev. B **53**, 7158 (1996).